PHYSICAL REVIEW B **90**, 134519 (2014)

Thermodynamics and existing phase of Ba-phenanthrene

Satoshi Heguri,[1,*] Quynh Thi Nhu Phan,[2] Yoichi Tanabe,[2] and Katsumi Tanigaki[1,2,†]
[1]*WPI-Advanced Institute for Materials Research (WPI-AIMR), Tohoku University, Sendai 980-8577, Japan*
[2]*Department of Physics, Tohoku University, Sendai 980-8577, Japan*

(Received 16 July 2014; revised manuscript received 3 October 2014; published 29 October 2014)

The thermodynaqmics for intercalation of phenanthrene (PHN) with Ba, for which superconductivity has been reported, is studied in comparison with its isomer of a linear aromatic hydrocarbon of anthracene (AN). Contrary to previous reports by other authors, the important observation that Ba is intercalated into neither PHN nor AN without affecting their molecular structures is unambiguously made by differential scanning calorimetry measurements and annealing time dependences observed by powder x-ray diffraction (XRD) measurements. The reactions of Ba and PHN at elevated temperatures lead this system to molecular decomposition instead of intercalation, resulting in the BaC_2 carbide or amorphous carbon formation, which is clearly supported by XRD and Raman spectroscopy. The phenomena of metallicity and superconductivity in PHN intercalated with alkaline-earth metals (Ba or Sr) should be reconsidered.

DOI: 10.1103/PhysRevB.90.134519 PACS number(s): 82.20.−w, 82.60.Hc, 79.60.Fr

I. INTRODUCTION

Since the discovery of K_3 (picene) superconductors with a superconducting transition temperature (T_C) of 7 and 18 K in 2010 [1], a large variety of aromatic hydrocarbon (AHC) superconductors have been reported, such as Rb_3 (picene), $Ca_{1.5}$ (picene), K_3 (picene), A_3 (PHN) (A = K, Rb), $E_{1.5}$PHN (E = Sr, Ba), R_1PHN (R = Sm, La), and K_3 (dibenzopentacene) with $T_C = 7$ K, 7 K, 3.5−15 K, 4.8−5 K, 5.4−5.6 K, 6.0−6.1 K, and 5−33 K, respectively [2–6]. Within this new family of AHC superconductors, the picene system has been studied with particular vigor, both experimentally and theoretically. In recent publications, arguments both for support of [6–8] and against [9–13] the existence of a superconducting phase are discussed, and a consensus has not yet been reached. A successful realization of the K_3 (picene) superconductor has been very difficult to repeat, since the superconducting shielding fraction of this system is generally too small to identify the actual superconducting phase. The observation of zero resistivity in the superconductivity of K_3 (picene) is much lower than the percolation limit [14] and presents an experimental problem. Unfortunately, there has been no guiding principle to improve the superconducting volume fraction until recently in the case of alkali-metal-doped AHCs. However, a high superconducting shielding fraction was reported recently for $E_{1.5}$ (PHN) (E = Sr and Ba) intercalations. In particular, $Ba_{1.5}$ (PHN) showed a sharp superconducting transition at 5.4 K with a shielding fraction of 65% [4]. Although the heat capacity measurements and analyses were retracted [15,16] due to a preparation problem with the sample, if the reports related to the synthesis are correct, PHN is then the most appropriate candidate to confirm the existence of superconducting AHCs and clarify the physical properties as well as the superconducting mechanism of AHC superconductors.

Another important question to be considered for these intercalated AHCs is the dependence of their homologous molecular structures on the occurrence of superconductivity, which is a very important issue in AHCs. Superconductivity has been reported so far only for armchair AHCs, such as picene and PHN, and no superconductivity has been reported for zigzag-type AHCs doped with alkali metals. We have recently conducted systematic research on anthracene (AN) doped with K and have confirmed that K_1AN is a Mott insulator; moreover, no metallic phase was found [17]. In both homologous AHCs the crystal symmetry and the electronic states are considered to be similar with each other, due to their monoclinic or triclinic low symmetric structure, resulting in a nondegenerate molecular orbital. In the case of graphene, the armchair or the zigzag edge structure is reported to have a large influence on the electronic states because a narrow-band Fermi surface appears only in the zigzag-type graphene edge states. It is a very intriguing and important scientific issue to compare isomers of AHCs from the viewpoint of intercalated AHCs, and to investigate conditions under which a Fermi surface can exist and what dependence is observed between the isomeric forms in AHCs.

In the present study, we select AN and PHN as typical AHCs with two geometric isomer structures, the former being a zigzag linear chain type and the latter being an armchair structure type, and study their Ba-intercalated compounds by focusing on the stoichiometry of $Ba_{1.5}$ (PHN/AN) as a target material. Various annealing conditions are employed to synthesize $Ba_{1.5}$ (PHN), and synthetic temperature dependences are studied by powder x-ray diffraction (XRD) measurements. Moreover, differential scanning calorimetry (DSC) is also used to provide supporting information on the thermodynamics of the intercalation processes. We will show that on the contrary to previous reports, both intercalated $Ba_{1.5}$ (PHN) and $Ba_{1.5}$ (AN) do not exist. Instead they form the same BaC_2 carbide from a molecule at relatively low temperatures through decomposition via hydrogen abstraction by Ba. The stability is different between the both parent molecules by first-principles molecular orbital calculations, where PHN is reported to be more stable than AN [2]. For both PHN and AN doped with Ba, no superconductivity was detected above 2 K. Our experimental data are very reproducible but contrast considerably with data from previous reports.

---

[*] heguri@sspns.phys.tohoku.ac.jp

[†] tanigaki@sspns.phys.tohoku.ac.jp

II. EXPERIMENTAL PROCEDURE

Sublimed PHN of over 99.5% purity (Sigma-Aldrich Co.) and Ba metal of 99.9% purity (Furuuchi Chemical Corp.) were used. The PHN was purified further by the sublimation method prior to use. The paraffin oil was removed from the surface of Ba metal using ligroin in an ultrasonic cleaner. After Ba metal was burnished in an argon (Ar) glove box (O_2, 0.1 ppm) by removing the oxidized surface, it was ground into powder using a file. The stoichiometric mixture of PHN and Ba (PHN:Ba = 1:1.5) was ground carefully using a mechanical mortar and then pressed into a pellet by a tool made from tungsten carbide. The pellet was sealed into a quartz tube after evacuation and heated at 503–1373 K for 5–260 h by an electric furnace in order to identify good experimental conditions.

The structure was studied by powder XRD measurements at room temperature using synchrotron radiation ($\lambda = 0.79817$ Å) at SPring-8 (BL02B2) and a Rigaku SmartLab equipped with a monochromator and a Cu K_α radiation source. The specimen was sealed in a glass capillary under vacuum. DSC measurements were made on about 8-mg powder samples using a TA Instruments DSC2920 calorimeter and Rigaku Thermo plus Evo2 DSC8230. Pristine materials and their mixtures with Ba were loaded in stainless steel sample pans and were hermetically sealed using a cover made of aluminum. The samples were heated and cooled at a rate of 5 K/min in a flow of pure Ar gas. For magnetization measurements Ba-PHN was sealed, together with helium gas at about 1×10^3 Pa to allow for thermal exchange, into a handmade quartz tube. The magnetic measurements were performed between 2 and 15 K under an applied magnetic field of 10 Oe using a Quantum Design MPMS-XL7 superconducting quantum interference device (SQUID) magnetometer.

In the present experiments, all preparations of XRD capillaries, sample pans for DSC measurements, and sample tubes for magnetic measurements were performed in an Ar glove box. When we seal XRD capillaries or SQUID tubes, the specimens are hermetically sealed without exposure to air. Sample pans of DSC measurements are cold welded with a lid by pressing together with a standard plunger tool. A similar procedure was used for studying alkali-metal-doped fullerides in the earlier experiments.

III. RESULTS AND DISCUSSION

A. DSC measurements

In order to confirm previous studies, exactly the same synthesis condition reported in the literature [4] was first used. After mixing, grinding, and pelletizing the mixtures of Ba powder and purified PHN inside an Ar glove box, thermal treatment was made at 503 K for 192 h with several intermittent grindings and pelletization in three times. After heating, the color of pellets initially changed. However, PHN melted and then solidified with the original transparent color of pristine PHN at the bottom of the quartz tube, while the Ba powder did not change and remained in the quartz tube. A tantalum crucible was used for heating in order to avoid reactions between Ba and the quartz tubes. However, no intercalation reactions occurred even under this thermal heating condition, contrary to the previous report as explained in the following paragraph.

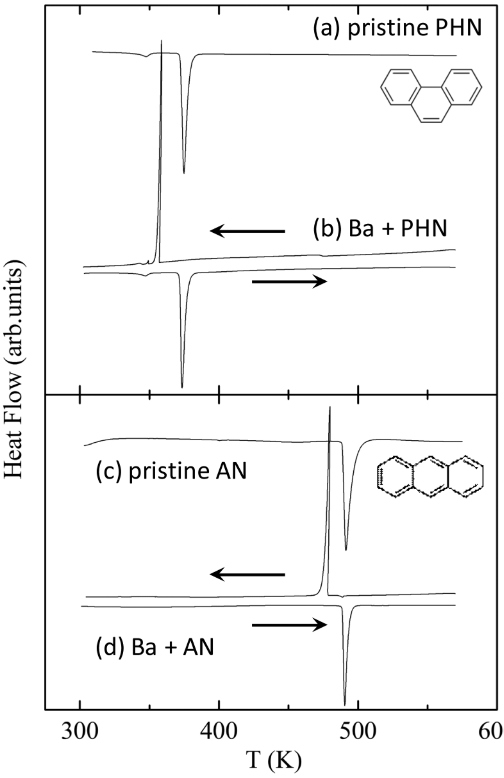

FIG. 1. Typical DSC thermodiagrams: (a) pristine PHN, (b) Ba + PHN, (c) pristine AN, and (d) Ba + AN. The arrows indicate scan direction of heating and cooling.

Figure 1 shows typical DSC thermo diagrams of pristine PHN and AN as well as their mixtures with Ba powder. Ba metal does not react with an Al hermetic pan below 600 K. The pristine PHN sample showed a clear endothermic peak at around 373 K, which corresponds to its melting point. As shown in Fig. 1(b), the Ba + PHN sample also showed an endothermic peak at the same temperature in the heating scan, which is indicative of a solid-liquid phase transition for PHN without any chemical reactions. It is important to note that the DSC scan showed no exothermic peaks associated with reactions between Ba powder and PHN at around 503 K, which was the temperature used for the synthesis in the previous report [4]. In the case of alkali-metal-doped C_{60}, an exothermic peak which can be attributed to a solid phase to form M_xC_{60} (M = Na, K, Rb, and Cs) intercalation compounds was reported in DSC measurements [18]. It is clear that both heating and cooling experiments indicate that any reactions between Ba and PHN do not occur even at 503 K, because the same spectrum showing the phase transition enthalpy of 88 J/g appeared in the scans of both directions. A similar behavior was observed for AN, as shown in Figs. 1(c) and 1(d). Only an endothermic peak at around 491 K, corresponding to the melting point of pristine AN, appeared in both measurements. These results unambiguously indicate that intercalation reactions do not occur between Ba and PHN/AN under the temperature region studied by DSC measurements.

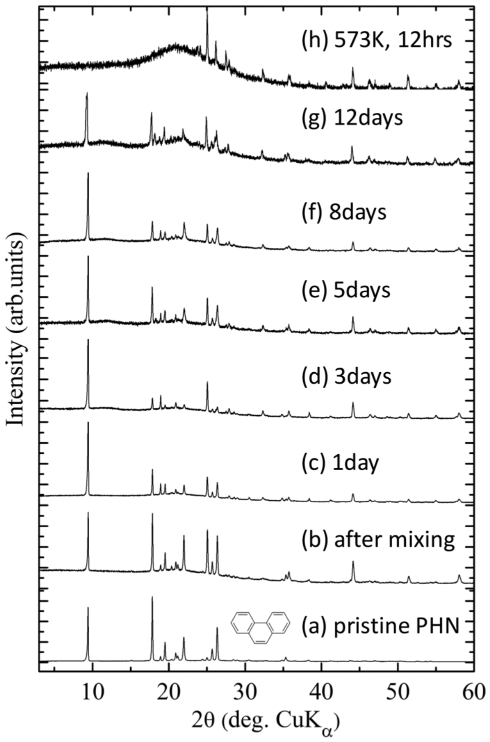

FIG. 2. Heating time dependencies of XRD profiles: (a) pristine PHN, (b) after mixing of Ba + PHN, (c)–(g) annealing time 1–12 days (as shown in figure), and (h) further annealing at 573 K for 12 h after 12 days annealing.

B. Annealing time dependence of XRD

The heating time dependences of XRD measurements were studied in order to acquire more detailed information about the reaction processes. The XRD profiles between PHN and Ba are shown in Fig. 2 as a function of heating time. The diffraction peak intensities are normalized to compare the new peaks appearing at higher angles. The peaks of pristine PHN can be indexed well in the space group of $P2_1$, yielding $a = 8.460, b = 6.1557, c = 9.4580$ Å, and $\beta = 98.0^\circ$, using the crystal structure in Ref. [4]. There were no new diffraction peaks originating from the intercalation phase between pristine PHN and Ba metal, although small changes in the relative intensity of diffraction peaks in the XRD profile can be seen. The heating was repeated several times according to the report [4]. However, each XRD profile can be explained well by considering pristine PHN and free Ba metal after mixing for 12 days with continuous heating [Fig. 3(a), $R_{wp} = 10.93\%$, $R_e = 3.85\%$], and no reactions occurred. Only a small change can be detected in their relative intensities. Almost all peak intensities significantly decreased except for the first peak of 001 reflection, which suggests that the crystal morphology of PHN is slightly modified in the solid-liquid phase transition by heating and cooling straddling the melting point of pristine PHN. This is a well-known polymorphism phenomenon for organic molecules. It is noted that the relative intensities of the XRD profile in the previous report for the superconducting Ba$_{1.5}$PHN is similar to the pristine PHN [4]. This result indicates that the PHN holds its crystal structure during the annealing. In the next step, further heating at higher temperatures was carried out at 573 K for 12 h. The diffraction profiles changed significantly after heating. Our Rietveld refinement indicated that free Ba metal, BaH$_2$, and BaO formed as new phases without intercalation reactions, and moreover, the PHN disappeared as shown in Fig. 3(b) ($R_{wp} = 5.17\%, R_e = 4.97\%$). A broad peak originating from amorphous phases appeared as a by-product at around $2\theta =$ 20 degrees. This clearly suggests that a PHN molecule is decomposed during the additional thermal treatment at high temperatures.

Figure 4 shows the heating time dependences of the XRD profiles for a mixture of AN and Ba. The diffraction profile of pristine AN can also be indexed using the crystal structure in Ref. [19]. The diffraction peak intensities are normalized in order to identify the new peaks. In a similar fashion to PHN, the crystallinity of AN decreased gradually with increasing heating time. After heating for 8 days, the diffraction profile was indexed to pristine AN, free Ba metal, and BaO [Fig. 3(c), $R_{wp} = 10.42\%$, $R_e = 3.85\%$). This is quite similar to the case of PHN. Independently of the different molecular shape of armchair and zigzag-type molecules, intercalation reactions did not occur under these thermal heating conditions for either of the isomers of AN and PHN.

As the next step, various thermal treatment conditions were employed to find suitable synthetic conditions for a Ba-PHN mixture system. Typical experimental conditions that were employed are listed in Table I. The chemical reactions of Ba and PHN did not proceed at temperatures lower than 773 K. When the temperature was set above 773 K, exothermic reactions gradually started thermodynamically and proceeded with time. This is very reasonable considering the vapor pressure of the intercalant. In the case of Ba-doped fullerenes and Ba graphite intercalation compounds (GICs), heating temperatures in the range of 773–923 K were employed in the early reports [20–22]. On the other hand, the same synthetic difficulties for GIC and fullerides with alkaline-earth metals are also known. High heating temperatures for initiating the intercalation reactions are necessary in the case of alkaline-earth metals, but amorphization and/or decomposition are induced simultaneously in the process [20,23,24,25], even if one could set the optimized temperature and the time. Therefore these works for similar compounds indicate that one should take special care with the annealing temperature, especially for when the parent materials have low melting points and/or high vapor pressures.

After annealing at higher temperatures, the color of the quartz tube changed to black due to the chemical reactions between Ba and the quartz tube, and finally the color of the specimen also changed from gray to black, being accompanied with a change in shape. The XRD profile of Ba-PHN compounds resulting from heating at 923 K for 5 h is shown in Fig. 3(d). The XRD profile became simpler than those under low-temperature heating conditions. All diffraction peaks can be assigned to BaC$_2$ carbide and BaO with $R_{wp} = 3.77\%$, $R_e = 2.16\%$. The diffraction peaks associated with PHN totally disappeared. This indicates that PHN cannot keep its molecular structure under such high-temperature heating. In the first reaction process between Ba and PHN leading to decomposition, it is postulated that Ba reacts with hydrogen at the position of high electron density of the highest occupied

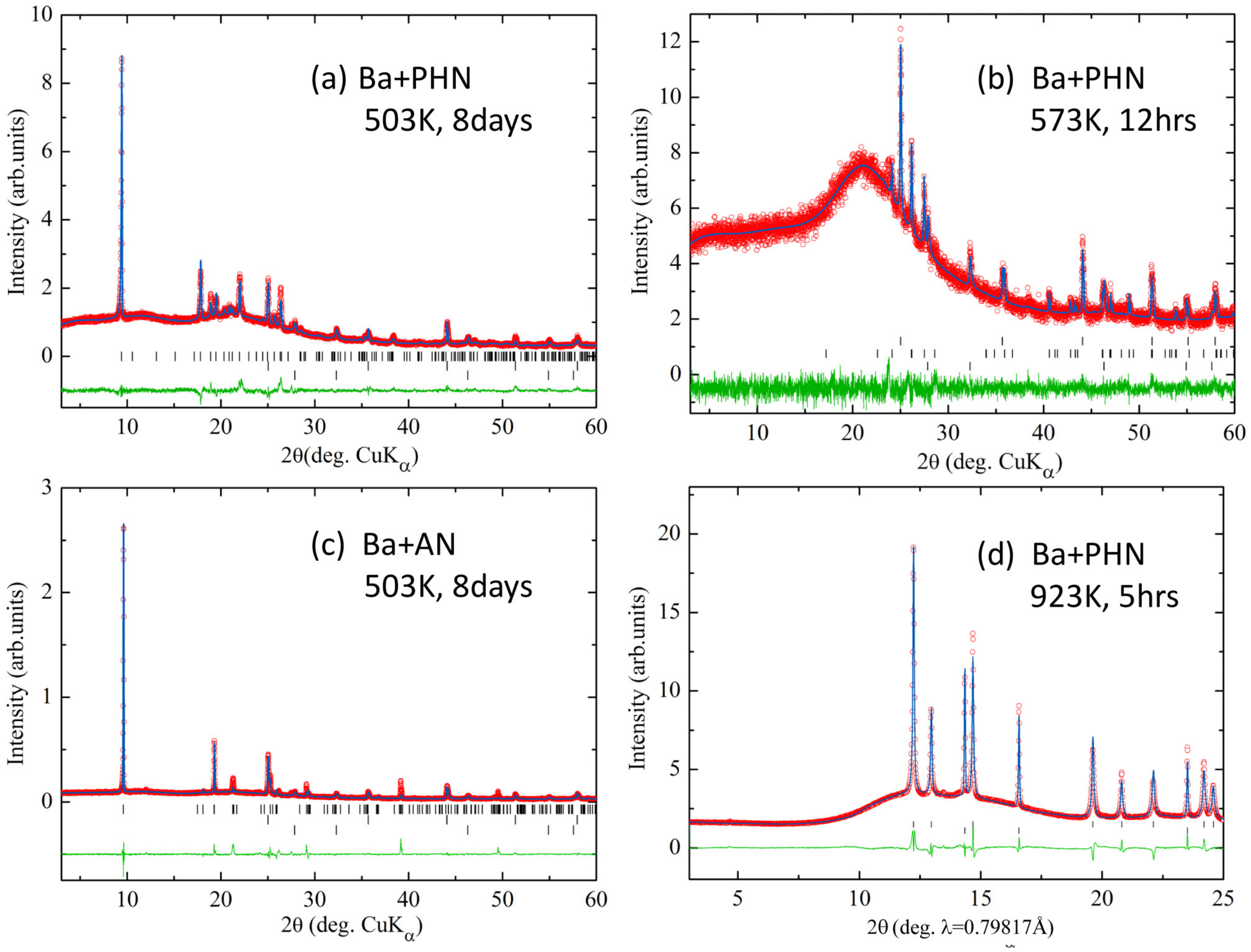

FIG. 3. (Color online) Experimental XRD profiles (red circles) and calculated (blue solid line) powder XRD profiles at ambient temperature under several annealing conditions: (a) Ba + PHN 8 days annealing, (b) Ba + PHN further annealing, (c) Ba + AN 8 days annealing, and (d) Ba + PHN high-temperature annealing at 923 K. The lower green solid lines are the differences and the tick marks show the reflection positions: (a) and (c) pristine PHN (top) and AN (top), free Ba metal (middle), and BaO (bottom); (b) free Ba metal (top), BaH_2 (middle), and BaO (bottom); (d) BaC_2 (top) and BaO (bottom).

molecular orbital (HOMO). After the occurrence of hydrogen abstraction reactions from PHN by Ba, the PHN molecule becomes unstable due to a collapse in the charge valance, and then Ba can easily make a chemical bond with the carbon of PHN, leading to carbide formation via decomposition of the PHN molecular structure. Finally, higher-temperature heating completely induces the molecular decomposition to produce BaC_2.

C. Raman spectra

The ambient temperature Raman spectra for pristine PHN and the nominal stoichiometric $Ba_{1.5}$ (PHN) heated under the condition of 503 K and 923 K are shown in Fig. 5. Several intense peaks for pristine PHN and $Ba_{1.5}$ (PHN) annealed at the reported temperature of 503 K for 8 days were observed at 1035, 1348, 1441, 1523, and 1623 cm^{-1}. These peaks are assigned to the a_1 mode of the C-C stretching vibration [26]. As for Ba-PHN annealed at 923 K, the Raman spectrum changed completely without a trace of pristine PHN peaks. All C-C stretching modes disappeared, and two significant peaks appeared at 1350 cm^{-1} and in the range of 1550–1570 cm^{-1}. These broad peaks are typically assigned to the D bands of crystalline nanographite or to an amorphous carbon phase [27], which clearly supports our conclusion that the PHN molecular structure decomposes under a high-temperature heating condition. In the case of low-temperature heating of PHN with Ba, Ba metals did not intercalate into the PHN lattice by employing the reported condition. According to reports on alkaline-earth-metal-doped fullerides, high temperature with a short time annealing in a solid-state reaction was claimed to be effective for making intercalations. However, only BaC_2 was produced from the decomposition of PHN in this system, as can apparently be concluded by XRD. This evidently indicates that there is no Ba-intercalated PHN phase under the described conditions.

D. Magnetic properties

In order to confirm superconductivity in all samples, magnetic susceptibility measurements for detecting superconducting diamagnetic signals were carried out using SQUID

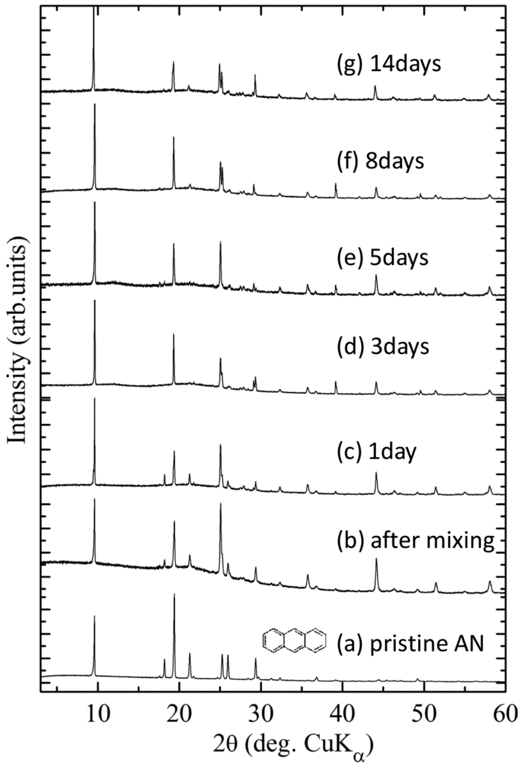

FIG. 4. Annealing time dependences of XRD profiles for (a) pristine AN, (b) after mixing of Ba + AN, (c)–(g) annealing time of 1–14 days (as shown in the figure).

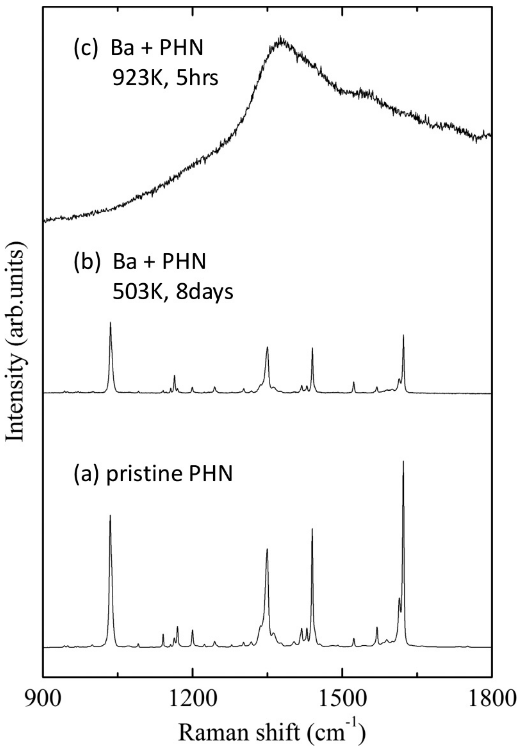

FIG. 5. Raman spectra: (a) pristine PHN, (b) Ba-PHN compound with heating at 503 K for 8 days, and (c) Ba-PHN compound with heating at 923 K for 5 h.

under an applied low magnetic field of 10 Oe. Figure 6 shows typical observed temperature dependences in zero-field cooling measurements for Ba-PHN specimens. No trace of superconductivity was found. In general, if there is a real superconducting phase, then one would expect to see at least a trace of superconductivity, because the superconducting diamagnetism is very large.

Figure 7 shows the phase diagrams for Ba metal, pristine PHN, and pristine AN under ambient pressure. Both pristine PHN and AN become liquid at 503 K; however, Ba metal is still solid due to its relatively high melting temperature compared to organic materials. A phase separation can easily occur between Ba and PHN/AN during thermal heating below 503 K. Both pristine PHN and AN are in a liquid phase and Ba is in a solid phase at 503 K, while the former two are in a vapor phase and Ba is in a liquid phase above 773 K. According to our experiments, a chemical reaction starts only at high temperatures, finally leading to the formation of BaC_2 carbide. Although the structure of the parent molecule should not decompose during an intercalation reaction process, similarly

TABLE I. Typical synthesis conditions for Ba_xPHN.

Composition x	Annealing temp. (K)	Annealing time (h)	Superconductivity above 2 K
1.5	503	48 + 72 + 72	×
1.5	503	48 + 48 + 48 + 48	×
1.5	503	48 + 144	×
1.5	503	72	×
1.5	503	192	×
1.5	773	240	×
1.5	823	5	×
1.5	923	5	×
1.5	1023	5	×
Excess	503	168	×
Excess	1373	10	×

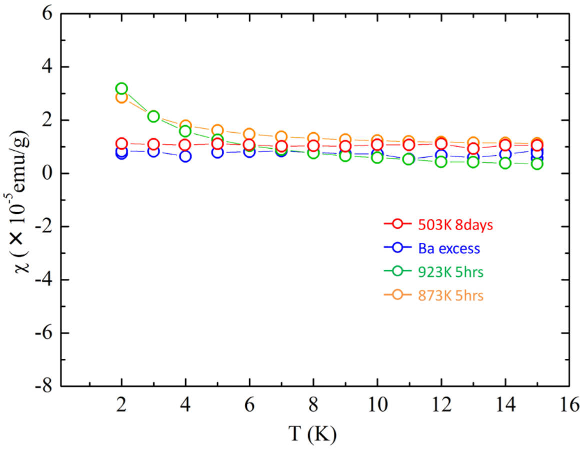

FIG. 6. (Color online) Temperature dependences of magnetic susceptibilities for typical Ba-PHN compounds. The annealing conditions are 503 K for 8 days (red), in an excess amount of Ba at 503 K for 168 h (blue), at 923 K for 5 h (green), and at 873 K for 5 h (orange). The detailed conditions are shown in Table I.

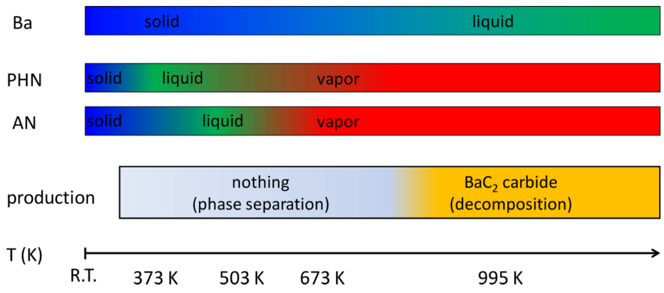

FIG. 7. (Color online) Phase diagrams for Ba metal, pristine PHN/AN, and their mixtures under ambient pressure.

to the case of fullerene and graphite with an alkaline-earth metal, such a molecular structural decomposition clearly starts in both PHN and AN under high-temperature heating, as described earlier. It is certainly impossible to synthesize the intercalation compounds of AN and PHN with Ba using a conventional solid-state reaction. In Ba-PHN/AN from the XRD studies, Ba metal easily abstracts hydrogen atoms and consequently, the molecules decompose without intercalation into a lattice, which instead leads to the formation of BaC_2 carbide. The activation energy for intercalation is considered to be much larger in the case of Sr-doped PHN [4], and therefore a similar phenomenon will occur at a higher temperature for Sr than that for Ba. Rare-earth metal-intercalated PHN superconductors have also been reported [6]. However, such a result is also yet to be independently confirmed. It is also important to note that recent density functional theory calculations by Naghavi *et al.* showed that the lowest energy state is not metallic but band insulating [28]. It would not be a scientifically reasonable situation for only one or two groups to continuously claim metallicity and superconductivity in bulk AHCs doped with alkali, alkaline-earth, as well as rare-earth metals.

IV. SUMMARY

Intercalation thermodynamics of PHN with Ba, an isomer of a linear aromatic hydrocarbon of AN, were studied. Various heating conditions were employed to synthesize Ba-PHN compounds, with a focus on the widely studied $Ba_{1.5}$ (PHN). First a procedure that was previously reported was repeated. However, no similar reactions occurred between Ba and PHN under a heating temperature of 503 K. Several higher-temperature conditions of 823–1373 K were also employed, and the only observed reactions were the formation of a carbide phase of BaC_2 via molecular decomposition. In the present studies, our careful experiments gave a completely different result from those reported previously. There were no intercalation phases existing thermodynamically in neither PHN nor its structurally analogous AN isomer with Ba. Moreover, no superconductivity was detected above 2 K in both Ba-PHN and Ba-AN systems. The true situation regarding metallicity and superconductivity in PHN intercalation with Ba or Sr should be reconsidered.

ACKNOWLEDGMENTS

The authors are grateful to M. Kobayashi for his useful comments and discussion. This research was partially supported by a Tohoku University GCOE program "Weaving Science Web beyond Particle-Matter Hierarchy," and a Grant in Aid for Scientific Research and World Premier International Research Center Initiative (WPI) from the MEXT of Japan. This work was supported by the Joint Studies Program of the Institute for Molecular Science.

---

[1] R. Mitsuhashi, Y. Suzuki, Y. Yamanari, H. Mitamura, T. Kambe, N. Ikeda, H. Okamoto, A. Fujiwara, M. Yamaji, N. Kawasaki, Y. Maniwa, and Y. Kubozono, Nature (London) **464**, 76 (2010).

[2] Y. Kubozono, H. Mitamura, X. Lee, X. He, Y. Yamanari, Y. Takahashi, Y. Suzuki, Y. Kaji, R. Eguchi, K. Akaike, T. Kambe, H. Okamoto, A. Fujiwara, T. Kato, T. Kosugi, and H. Aoki, Phys. Chem. Chem. Phys. **13**, 16476 (2011).

[3] X. Wang, R. Liu, Z. Gui, Y. Xie, Y. Yan, J. Ying, X. Luo, and X. Chen, Nat. Commun. **2**, 507 (2011).

[4] X. F. Wang, Y. J. Yan, Z. Gui, R. H. Liu, J. J. Ying, X. G. Luo, and X. H. Chen, Phys. Rev. B **84**, 214523 (2011).

[5] M. Xue, T. Cao, D. Wang, Y. Wu, H. Yang, X. Dong, J. He, F. Li, and G. F. Chen, Sci. Rep. **2**, 389 (2012).

[6] X. F. Wang, X. G. Luo, J. J. Ying, X. J. Xiang, S. L. Zhang, R. R. Zhang, Z. H. Zhang, Y. J. Yan, A. F. Wang, P. Cheng, G. L. Ye, and X. H. Chen, J. Phys.: Condens. Matter. **24**, 345701 (2012).

[7] H. Okazaki, T. Wakita, T. Muro, Y. Kaji, X. Lee, H. Mitamura, N. Kawasaki, Y. Kubozono, Y. Yamanari, T. Kambe, T. Kato, M. Hirai, Y. Muraoka, and T. Yokoya, Phys. Rev. B **82**, 195114 (2010).

[8] T. Kato, T. Kambe, and Y. Kubozono, Phys. Rev. Lett. **107**, 077001 (2011).

[9] M. Casula, M. Calandra, G. Profeta, and F. Mauri, Phys. Rev. Lett. **107**, 137006 (2011).

[10] A. Ruff, M. Sing, R. Claessen, H. Lee, M. Tomić, H. O. Jeschke, and R. Valentí, Phys. Rev. Lett. **110**, 216403 (2013).

[11] B. Mahns, F. Roth, and M. Knupfer, J. Chem. Phys. **136**, 134503 (2012).

[12] A. Takahashi, H. Itoh, and M. Aihara, Phys. Rev. B **77**, 205105 (2008).

[13] M. Caputo, G. Di Santo, P. Parisse, L. Petaccia, L. Floreano, A. Verdini, M. Panighel, C. Struzzi, B. Taleatu, C. Lal, and A. Goldoni, J. Phys. Chem. C **116**, 19902 (2012).

[14] K. Teranishi, X. He, Y. Sakai, M. Izumi, H. Goto, R. Eguchi, Y. Takabayashi, T. Kambe, and Y. Kubozono, Phys. Rev. B **87**, 060505 (2013).

[15] J. Ying, X. Wang, Y. Yan, Z. Xiang, X. Luo, Z. Sun, and X. Chen, Phys. Rev. B **87**, 179901 (2013).

[16] Y. Kasahara, Y. Takeuchi, and Y. Iwasa, Phys. Rev. B **87**, 179902(E) (2013).

[17] Q. T. N. Phan, S. Heguri, Y. Tanabe, H. Shimotani, T. Nakano, Y. Nozue, and K. Tanigaki, Dalton Trans. **43**, 10040 (2014).

[18] H. S. Chen, A. R. Kortan, R. C. Haddon, and N. Kopylov, J. Phys. Chem. **97**, 3088 (1993).

[19] A. Charlesby, G. Finch, and H. Willman, Proc. Phys. Soc. **51**, 479 (1939).

[20] C. M. Brown, S. Taga, B. Gogia, K. Kordatos, S. Margadonna, K. Prassides, Y. Iwasa, K. Tanigaki, A. N. Fitch, and P. Pattison, Phys. Rev. Lett. **83**, 2258 (1999).

[21] S. Nakamae, A. Gauzzi, F. Ladieu, D. L'Hote, N. Emery, C. Herold, J. F. Mareche, P. Lagrange, and G. Loupias, Solid State Commun. **145**, 493 (2008).

[22] S. Heguri and M. Kobayashi, J. Phys. Chem. Solids **71**, 572 (2010).

[23] S. Heguri, T. Hara, and M. Kobayashi, Solid State Commun. **148**, 251 (2008).

[24] S. Heguri and M. Kobayashi, Solid State Commun. **150**, 1489 (2010).

[25] S. Heguri and M. Kobayashi, Chem. Phys. Lett. **490**, 34 (2010).

[26] J. M. L. Martin, J. E. Yazal, and J. P. Francois, J. Phys. Chem. **100**, 15358 (1996).

[27] J. R. Patterson, S. A. Catledge, and Y. K. Vohra, Appl. Phys. Lett. **77**, 851 (2001).

[28] S. S. Naghavi, M. Fabrizio, T. Qin, and E. Tosatti, Phys. Rev. B **88**, 115106 (2013).